NASA TECHNICAL NOTE

NASA TN D-8089
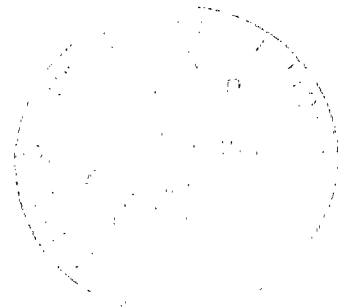
NASA TN D-8089

FREE-FLIGHT MODEL INVESTIGATION
OF A VERTICAL-ATTITUDE VTOL FIGHTER
WITH TWIN VERTICAL TAILS

Sue B. Grafton and Ernie L. Anglin

Langley Research Center
Hampton, Va. 23665

NATIONAL AERONAUTICS AND SPACE ADMINISTRATION • WASHINGTON, D. C. • NOVEMBER 1975

1. Report No. NASA TN D-8089	2. Government Accession No.	3. Recipient's Catalog No.
4. Title and Subtitle FREE-FLIGHT MODEL INVESTIGATION OF A VERTICAL-ATTITUDE VTOL FIGHTER WITH TWIN VERTICAL TAILS		5. Report Date November 1975
		6. Performing Organization Code
7. Author(s) Sue B. Grafton and Ernie L. Anglin		8. Performing Organization Report No. L-10450
9. Performing Organization Name and Address NASA Langley Research Center Hampton, Va. 23665		10. Work Unit No. 505-06-98-01
		11. Contract or Grant No.
12. Sponsoring Agency Name and Address National Aeronautics and Space Administration Washington, D.C. 20546		13. Type of Report and Period Covered Technical Note
		14. Sponsoring Agency Code

15. Supplementary Notes

Technical Film Supplement L-1167 available on request.

16. Abstract

Free-flight tests were conducted in the Langley full-scale tunnel to determine the stability and control characteristics of a vertical-attitude VTOL fighter having twin vertical tails and a pivoted fuselage forebody (nose-cockpit) arrangement. The flight tests included hovering flights and transition flights from hover to conventional forward flight. Static force tests were also made to aid in the analysis of the flight tests. The model exhibited satisfactory stability and control characteristics, and the transition from hovering flight to conventional forward flight was relatively smooth and straightforward.

17. Key Words (Suggested by Author(s)) VTOL Static and dynamic force tests Free-flight tests	18. Distribution Statement Unclassified — Unlimited Subject Category 02		
19. Security Classif. (of this report) Unclassified	20. Security Classif. (of this page) Unclassified	21. No. of Pages 28	22. Price* $3.75

*For sale by the National Technical Information Service, Springfield, Virginia 22161

FREE-FLIGHT MODEL INVESTIGATION OF A VERTICAL-ATTITUDE
VTOL FIGHTER WITH TWIN VERTICAL TAILS

Sue B. Grafton and Ernie L. Anglin
Langley Research Center

SUMMARY

Free-flight tests were made using a model of a vertical-attitude VTOL fighter with a pivoted fuselage forebody (nose-cockpit) design with twin vertical tails. The tests were conducted in the Langley full-scale tunnel and included an investigation of (1) dynamic stability characteristics at several attitudes during the transition from hovering to forward flight, (2) the lateral-directional control power required to hover, and (3) the need for artificial rate damping. Static force tests were also conducted to aid in the analysis of the flight tests.

Results of the investigation showed that the model was neutrally stable in hovering flight and quite sensitive to control inputs, but relatively smooth transitions could be made to conventional forward flight without artificial stabilization. The model exhibited satisfactory longitudinal and lateral-directional stability in all flight tests without artificial stabilization. With artificial dampers operating, transitions could be achieved with a minimum of pilot effort and control.

INTRODUCTION

During the early 1950's, considerable interest was expressed in vertical-attitude VTOL fighter configurations. The free-flight model test program for the delta-wing X-13 research vehicle (ref. 1) demonstrated the ability of such configurations to complete transitions between hovering and forward flight in a relatively simple, straightforward manner. VTOL fighters of this type involve less compromise of the normal forward flight configuration to accommodate VTOL operation than do the various horizontal-attitude concepts that have been studied. However, the vertical-attitude VTOL concept was not developed into an operational aircraft at that time for a number of reasons, including:

(1) The thrust required for VTOL was so much greater than that demanded by any conventional flight requirement, that the additional engine size caused unacceptable losses in payload and range.

(2) The necessity of an elaborate ground apparatus for take-off and landing was considered operationally unacceptable.

(3) The vertical attitude of the cockpit during low-speed VTOL operations resulted in objectionable pilot attitudes which were judged to be unacceptable for an operational environment, particularly during landing.

As a result of these shortcomings, interest in the concept greatly diminished.

Recently, however, advances in fighter requirements and technology have resulted in configuration features which may minimize or even eliminate some of the previous shortcomings of vertical-attitude VTOL vehicles. For example, recent lightweight fighter prototypes have uninstalled thrust-weight ratios of about 1.5, this level of thrust being required to meet the combat performance requirements. Also available are fly-by-wire control systems which eliminate control linkage problems and can be incorporated in variable-geometry designs which eliminate the problem of pilot attitude variations. These features suggest the possibility of a vertical-attitude VTOL fighter which is essentially a conventional airplane having a conventional landing gear which can be used whenever a conventional landing is possible. Added features needed for VTOL operations would be a jet-reaction control system for control in hover and at low speeds, a landing hook for vertical landing on an apparatus such as that used for the X-13, and a pivoted nose-cockpit section so that the pilot could remain in a normal attitude as the airplane tilted to a vertical attitude for take-off and landing. The fly-by-wire control system would greatly facilitate this latter design feature as well as provide any particular control phasing required during the transition. Recently, free-flight model tests were conducted to investigate the dynamic stability and control characteristics of two configurations of this type. Reference 2 presents results of one of these investigations.

The present investigation was conducted to study the dynamic stability and control characteristics of a free-flight model of another vertical-attitude VTOL fighter having a pivoted fuselage forebody and twin vertical tails. Figure 1 shows a sketch of the concept under discussion. The investigation was conducted in the Langley full-scale tunnel and included hovering and transition flight tests and static force tests. The flight tests included an investigation of: (1) stability characteristics at several attitudes during the transition from hovering to forward flight, (2) the lateral-directional control power required to hover, and (3) the need for artificial rate damping.

Selected scenes from a motion picture of the free-flight tests have been prepared as a film supplement available on loan. A request card and a description of the film (L-1167) are included at the back of this report.

SYMBOLS

All longitudinal forces and moments are referred to the wind-axis system and the lateral-directional forces and moments are referred to the body-axis system shown in figure 2. All data are presented with respect to a center of gravity located at 25 percent of the wing mean aerodynamic chord. Dimensional quantities are presented both in the International System of Units (SI) and in U.S. Customary Units, and equivalent dimensions were determined by using the conversion factors given in reference 3.

b	span, m (ft)
c	local wing chord, m (ft)
$\bar{c}$	mean aerodynamic chord, m (ft)
C_D	drag coefficient, F_D/qS
C_L	lift coefficient, F_L/qS
C_l	rolling-moment coefficient, M_X/qSb
C_m	pitching-moment coefficient, $M_Y/qS\bar{c}$
C_n	yawing-moment coefficient, M_Z/qSb
C_Y	side-force coefficient, F_Y/qS
F_D	drag force, N (lb)
F_L	lift force, N (lb)
F_Y	side force, N (lb)
I_X	moment of inertia about X body axis, $kg\text{-}m^2$ ($slug\text{-}ft^2$)
I_Y	moment of inertia about Y body axis, $kg\text{-}m^2$ ($slug\text{-}ft^2$)

I_Z moment of inertia about Z body axis, $kg\text{-}m^2$ $(slug\text{-}ft^2)$

M_X rolling moment, $m\text{-}N$ $(ft\text{-}lb)$

M_Y pitching moment, $m\text{-}N$ $(ft\text{-}lb)$

M_Z yawing moment, $m\text{-}N$ $(ft\text{-}lb)$

q free-stream dynamic pressure, N/m^2 (lb/ft^2)

S wing area, m^2 (ft^2)

α angle of attack of fuselage, deg

β angle of sideslip, deg

δ_a aileron deflection (per surface), positive for left roll, deg

δ_h horizontal-tail deflection, positive when trailing-edge is down, deg

δ_n fuselage forebody-deflection angle, positive for nose down from fuselage reference line (see fig. 1), deg

δ_r rudder deflection, positive for left yaw, deg

ΔC_l incremental rolling-moment coefficient

ΔC_n incremental yawing-moment coefficient

ΔC_Y incremental side-force coefficient

$$C_{l_\beta} = \frac{\partial C_l}{\partial \beta} \qquad\qquad C_{n_\beta} = \frac{\partial C_n}{\partial \beta} \qquad\qquad C_{Y_\beta} = \frac{\partial C_Y}{\partial \beta}$$

$$C_{n_{\beta,dyn}} = C_{n_\beta} - \frac{I_Z}{I_X} C_{l_\beta} \sin \alpha$$

4

MODEL, APPARATUS, AND TESTING TECHNIQUE

Model and Apparatus

The model configuration used in this investigation was intended to represent a vertical-attitude type of VTOL configuration (similar to the X-13) which could land and take off vertically from a landing platform. In this concept, a hook located near the nose gear of the vehicle engages a horizontal supporting member, or wire, on the platform for launch and recovery. After a vertical landing, the platform would be rotated to a horizontal position, and the vehicle would roll off on conventional landing gear.

The model was a modified version of an existing research model generally representative of current fighter configurations. A three-view sketch of the model is presented in figure 3, photographs of the model are presented in figure 4, and mass and geometric characteristics of the model are presented in table I. The model was of molded fiberglass construction, and the wing leading-edge flaps were deflected 25°. The landing platform was represented by a sheet of plywood, and the model-supporting member consisted of a 1.27-cm (1/2-in.) metal bar attached to the platform with brackets (fig. 4(a)).

The entire fuselage forebody including the cockpit was pivoted to permit 90° of nose-down rotation relative to the fuselage. This rotation caused small changes in the moments of inertia; examples at three fuselage forebody-deflection angles are presented in table I. The angular position of the nose was remotely controlled by an electric motor.

Power for thrust was obtained from compressed air which was brought into the top of the model (see fig. 4(b)) by flexible plastic tubing attached near the center of gravity. The air was ejected from multitube ejectors which exhausted out of the engine nozzle exits. This propulsive arrangement was used to promote additional mass flow into the open engine inlets and the auxiliary engine inlets. (See fig. 3.)

The longitudinal controls consisted of an all-movable horizontal tail and a jet-reaction control mounted at the rear of the fuselage, lateral controls consisted of aileron surfaces on the wing and jet-reaction controls mounted at each wing tip, and the directional controls were conventional rudders and a jet-reaction control mounted at the rear of the fuselage. The amount of control moment produced by the jet-reaction controls could be changed by varying the compressed-air pressure. The controls were actuated by electropneumatic servos which provided a full-on or full-off flicker-type deflection. The control surfaces and the associated jet-reaction controls were interconnected so that the control surfaces moved whenever the jet-reaction controls were actuated. Thus, the control power used during transition was a combination of the aerodynamic and jet-reaction controls. Each actuator had a motor-driven trimmer which was electrically operated by the pilots so that controls could be rapidly trimmed independently of the

flicker controls. The model was equipped with individual rate-damper systems for each axis which could be turned on and off separately. The rate dampers consisted of compressed-air-driven rate gyroscopes that actuated the control servos in proportion to roll rate, yaw rate, and pitch rate. The following control surface deflections were used during the flights:

Control deflection	Pilot (flicker)	Damper (proportional system, maximum deflection)
δ_h, deg	±9	±5
δ_a, deg	±18	±5
δ_r, deg	±23	±4

Free-Flight Test Technique

The typical test setup for the free-flight tests is shown in figure 5. The model was flown without restraint in the 9- by 18-m (30- by 60-ft) open-throat test section of the Langley full-scale tunnel and remotely controlled about all three axes by human pilots. Three pilots were used during the tests. The two pilots who controlled the model about its roll and yaw axes were located in an enclosure at the rear of the test section while the third pilot, who controlled the model in pitch, was stationed at one side of the tunnel. The lateral controls for hovering and for the first 30° of transition were provided by the roll and yaw pilots. However, lateral control for the remainder of the transition into forward flight was provided solely by the yaw pilot (rudder alone). Operators were also stationed at the side of the tunnel to control the model power, the safety cable, and the fuselage forebody-deflection angle. Pneumatic and electric power and control signals were supplied to the model through a flexible trailing cable which was made up of wires and light plastic tubes. The cable also incorporated a 0.318-cm (1/8-in.) steel cable that passed through a pulley above the test section. This element of the flight cable was used to restrain the model when an uncontrollable motion or mechanical failure occurred. The entire flight cable was kept slack during the flights by a safety-cable operator by use of a high-speed pneumatic winch. A further discussion of the free-flight technique, including the reasons for dividing the piloting tasks, is given in reference 4.

TESTS

Free-Flight Tests

The investigation consisted of free-flight tests to study the dynamic stability and control characteristics of the model over the speed range from hovering to forward flight.

The flights began with a vertical take-off from the landing platform, included a transition wherein the cockpit remained essentially horizontal until $\alpha \approx 30^{\circ}$, and ended with the model in conventional forward flight at high angles of attack (minimum $\alpha = 25^{\circ}$) with $\delta_n = 0^{\circ}$. The tests included steady flights at several speeds, an examination of the control power used during the transition, and an evaluation of the need for artificial rate damping. Results of the flight tests were mainly qualitative and consisted of pilot opinions of the overall behavior of the model.

Motion-picture records were made of all flights and selected scenes are included in a film supplement to this report.

Force Tests

Static force tests were conducted in the Langley full-scale tunnel at a Reynolds number of 0.8×10^6 based on the mean aerodynamic chord of the wing. These tests were made to determine the aerodynamic characteristics of the model and to determine values of static stability derivatives for use in analysis and interpretation of the free-flight tests. The forebody-deflection angle δ_n was varied from 0° (alined with fuselage reference line) in increments of 10°. At each fuselage forebody-deflection angle, tests were made over an angle-of-attack range as follows:

δ_n, deg	α range, deg
0	0 to 20
10	0 to 20
20	10 to 30
30	20 to 40
40	30 to 50
50	40 to 60
60	50 to 70
70	60 to 80
78	70 to 97.5

Note that the middle angle of attack of each range (except for $\delta_n = 0^{\circ}$) is where $\delta_n = \alpha$. As a result, the local angle of attack at the nose was 0°. Thus, the test condition represented a point during a level-flight transition. The range of angle of attack was then repeated for the various angles of sideslip from -5° to 5°. Tests were also conducted to determine the aileron and rudder effectiveness of the configuration for angles of attack from 0° to 90° at $\beta = 0^{\circ}$.

The forces and moments were measured on a six-component internal strain-gage balance, and the model was mounted on a strut that entered the top of the fuselage just behind the center of gravity.

Conventional wind-tunnel corrections for flow angularity have been applied to all force-test data presented herein. No wall corrections were applied because of the very small size of the model relative to that of the tunnel test section.

RESULTS OF FORCE TESTS

The force tests were not the principal objective of the investigation, but these tests were made to determine the aerodynamic characteristics of the model and to determine values of static stability derivatives for use in analysis and interpretation of the free-flight tests.

As mentioned previously, the data were measured in tests defined by the fuselage forebody-deflection angle δ_n which is used in the keys of the data figures.

Static Longitudinal Stability

The static longitudinal characteristics of the model are presented in figure 6. Since the data show that the model was longitudinally stable throughout the range of angle of attack, deflecting the nose had a negligible effect on the static longitudinal characteristics. These results indicate that the model should exhibit satisfactory longitudinal stability in free flight; this hypothesis was subsequently verified by the flight tests.

Static Lateral-Directional Stability

The static lateral-directional characteristics of the model are presented in figure 7 in terms of the static lateral-directional stability derivatives C_{Y_β}, C_{n_β}, and C_{l_β}. The values of the derivatives were based on measurements obtained for an angle-of-sideslip range of $\pm 5^o$. The data of figure 7 indicate that the model had positive (stable) values of C_{n_β} at low angles of attack (below $\alpha = 23^o$), small unstable values between $\alpha = 23^o$ and $\alpha = 27^o$, and generally large unstable values beyond $\alpha = 35^o$. The data also show that fuselage forebody-deflection angle had no significant effect on directional stability or on the effective dihedral derivative C_{l_β}. In addition, the effective dihedral derivative increased $\left(-C_{l_\beta}\right)$ as α was increased to about 20° where a large reduction in $-C_{l_\beta}$ began. The magnitude of $-C_{l_\beta}$ became very unstable near $\alpha = 40^o$, the same angle at which C_{n_β} reached a minimum. The loss of directional stability and effective dihedral which occurred near maximum lift ($\alpha = 35^o$) can promote directional divergence as discussed in reference 5.

Lateral-Directional Control Characteristics

Results of the tests to determine control effectiveness of the rudder and ailerons are presented in figures 8 and 9 in terms of the incremental values of C_l, C_n, and C_Y produced by a right-yaw or right-roll control.

Figure 8 shows the incremental forces and moments produced by rudder deflection for a right-yaw control. The data show that the effectiveness of the rudders for yaw control decreased above $\alpha = 15^\circ$ and was fairly constant up to $\alpha = 40^\circ$. The rudders were also effective for roll control between $\alpha = 30^\circ$ and $\alpha = 40^\circ$.

Shown in figure 9 are the values of ΔC_Y, ΔC_n, and ΔC_l produced by aileron deflection for right-roll control. The data show that the effectiveness of the ailerons decreased rapidly between $\alpha = 10^\circ$ and $\alpha = 35^\circ$ and that aileron deflection produced adverse yawing moments above $\alpha = 18^\circ$. The magnitude of adverse yawing moments increased beyond $\alpha = 45^\circ$.

RESULTS AND DISCUSSION OF FLIGHT TESTS

A motion-picture film supplement with selected scenes from the free-flight tests has been prepared and is available on loan. A request card and a description of the film are found at the back of this report.

Longitudinal Characteristics

As mentioned previously, most tests were made as continuous flights from hovering to conventional forward flight (minimum $\alpha = 25^\circ$). All the free-flight tests were made for a center of gravity at $0.25\bar{c}$. The results of the investigation showed that the model was neutrally stable in hovering flight, and without artificial rate dampers it was extremely sensitive to control inputs. Even without artificial rate damping, however, transitions could be made from hover to normal forward flight with no significant problem to the pitch pilot, except for the necessity of maintaining careful attention to the change of trim through the transition. The longitudinal stability and control was satisfactory, as would be expected on the basis of results of the force tests.

Lateral-Directional Characteristics

In hovering flight without artificial stabilization, the model was extremely sensitive to roll and yaw control inputs. During the transition tests the model was easy to fly, and the pilot was able to make relatively smooth transitions from hovering to forward flight without artificial stabilization. The pilot did notice a slight tendency to diverge in yaw around $\alpha = 40^\circ$. With roll and yaw dampers on, the model had no noticeable tendency to diverge in yaw and could perform smooth transitions with a minimum pilot effort.

The tendency of the unaugmented model to diverge in yaw can be predicted on the basis of a criterion known as $C_{n_\beta,dyn}$ which has been used in past investigations to evaluate the effects on dynamic stability of lateral and directional stability, angle of attack, and inertial distribution. In particular, past studies have shown that negative values of $C_{n_\beta,dyn}$ indicate a tendency toward divergence in yaw (see ref. 5) where

$$C_{n_\beta,dyn} = C_{n_\beta} - \frac{I_Z}{I_X} C_{l_\beta} \sin \alpha$$

Presented in figure 10 are the values of $C_{n_\beta,dyn}$ based on the force-test data of figure 7 for fuselage forebody-deflection angles of 0° and 78°. The data show that $C_{n_\beta,dyn}$ reached large negative values near $\alpha = 40^o$. The divergence encountered in flight was a result of the large unstable values of C_{n_β} and C_{l_β} indicated in figure 7.

Evaluation of Lateral-Directional Control Power Required in Hover

It is recognized that the minimum control power needed to control the model in hover using the free-flight model technique would probably not correspond to minimum control power required by a pilot of a full-scale airplane because of the remote model-pilot location and rapidity of model motions. Therefore, no attempt has been made to correlate the values of control power required to fly the model with values recommended for satisfactory handling qualities of a full-scale airplane. However, shown in the follow-ing table are the values of minimum control power (scaled up to full-scale) required by the pilots to maintain control of the model in hovering flight. The values, which are pre-sented in relation to the axis system perceived by the on-board pilot seated in the hori-zontal forebody, were obtained from calibrations of the jet-reaction controls using the minimum air-pressure level determined in the tests and were then scaled up to full-scale on the basis of an aircraft weight of 88 075 N (19 800 lb).

Parameter	Dampers	
	Off	On
$\frac{\text{Roll-control moment}}{\text{Inertia}}$, radians/sec^2 . . .	0.103	0.053
$\frac{\text{Yaw-control moment}}{\text{Inertia}}$, radians/sec^2 . . .	.540	.346

The data in the table show that with the rate dampers off, the control power needed for satisfactory flights was substantially higher than with the rate dampers operating. It

is quite probable that the amount of jet-reaction control could have been reduced as the transition from hovering to normal forward flight progressed, but no attempt was made to determine the minimum control power needed at each angle of attack.

More sophisticated analysis techniques, such as piloted simulation, are required to obtain quantitative information on the flying qualities and control power required for a full-scale configuration. In addition, critical operational maneuvers, such as the vertical landing, were considered to be beyond the scope of the present study.

SUMMARY OF RESULTS

Results of a free-flight model investigation to determine the dynamic stability and control characteristics of a vertical-attitude VTOL fighter airplane with a pivoted fuselage forebody (nose-cockpit) design and twin vertical tails may be summarized as follows:

1. In hovering flight without artificial stabilization, the model was neutrally stable and extremely sensitive to control inputs, but relatively smooth transitions to conventional forward flight could be made with suitable attention to the controls.

2. The model exhibited satisfactory longitudinal stability in all flight tests.

3. Without artificial stabilization, the model exhibited a slight tendency to diverge in yaw around an angle of attack of 40°.

4. With artificial stabilization, very smooth transitions from hovering to normal forward flight could consistently be made with little effort.

5. Rate dampers decreased the amount of control power used by the roll and yaw pilots.

Langley Research Center
National Aeronautics and Space Administration
Hampton, Va. 23665
September 23, 1975

REFERENCES

1. Smith, Charles C., Jr.: Hovering and Transition Flight Tests of a 1/5-Scale Model of a Jet-Powered Vertical-Attitude VTOL Research Airplane. NASA TN D-404, 1961. (Supersedes NASA MEMO 10-27-58L.)

2. Newsom, William A., Jr.; and Anglin, Ernie L.: Free-Flight Model Investigation of a Vertical-Attitude VTOL Fighter. NASA TN D-8054, 1975.

3. Mechtly, E. A.: The International System of Units – Physical Constants and Conversion Factors (Second Revision). NASA SP-7012, 1973.

4. Parlett, Lysle P.; and Kirby, Robert H.: Test Techniques Used by NASA for Investigating Dynamic Stability Characteristics of V/STOL Models. J. Aircraft, vol. 1, no. 5, Sept.-Oct. 1964, pp. 260-266.

5. Chambers, Joseph R.; and Anglin, Ernie L.: Analysis of Lateral-Directional Stability Characteristics of a Twin-Jet Fighter Airplane at High Angles of Attack. NASA TN D-5361, 1969.

TABLE I.- MASS AND GEOMETRIC CHARACTERISTICS OF MODEL

Weight, N (lb) 296.92 (66.75)

Moments of inertia:

	Fuselage forebody-deflection angle of −		
	0°	45°	78°
I_X, kg-m^2 (slug-ft^2)	0.845 (0.623)	0.944 (0.696)	1.335 (0.985)
I_Y, kg-m^2 (slug-ft^2)	7.069 (5.214)	6.969 (5.140)	6.904 (5.092)
I_Z, kg-m^2 (slug-ft^2)	7.862 (5.799)	7.854 (5.793)	7.513 (5.541)

Overall fuselage length, m (ft) 2.40 (7.88)

Wing:

Span, m (ft) 1.60 (5.25)

Area, m^2 (ft^2) 0.73 (7.88)

Root chord, m (ft) 0.68 (2.23)

Tip chord, m (ft) 0.24 (0.78)

Mean aerodynamic chord, m (ft) 0.494 (1.62)

Aspect ratio 3.5

Taper ratio 0.35

Sweepback of 0.25c, deg 20

Sweepback of leading edge, deg 26.6

Dihedral, deg . . . . −5

Horizontal tail:

Area (exposed), m^2 (ft^2) 0.18 (1.91)

Span (exposed), m (ft) 0.73 (2.40)

Root chord, m (ft) 0.30 (1.00)

Tip chord, m (ft) 0.18 (0.60)

Sweepback of 0.25c, deg 38

Taper ratio 0.6

TABLE I.- Concluded

Aspect ratio 3.0
Mean aerodynamic chord, m (ft) 0.25 (0.82)
Tail length, 0.25c̄ of wing to 0.25c̄ of tail, m (ft) 0.80 (2.64)
Dihedral, deg . . . . -2
Volume coefficient 0.396

Vertical tails:
    Area (per side), m² (ft²). 0.11 (1.17)
    Span, m (ft) 0.36 (1.19)
    Root chord, m (ft) 0.43 (1.41)
    Tip chord, m (ft) 0.17 (0.56)
    Sweepback of 0.25c, deg. 35
    Taper ratio 0.40
    Aspect ratio 1.21
    Mean aerodynamic chord, m (ft) 0.32 (1.05)
    Tail length, 0.25c̄ of wing to 0.25c̄ of tail, m (ft) 0.49 (1.61)
    Cant angle, deg 20
    Toe out, deg 1

Aileron:
    Area (per side), m² (ft²) 0.017 (0.185)
    Hinge-line location, percent chord 70

Rudder:
    Area (per side), m² (ft²) 0.018 (0.191)
    Hinge-line location, percent chord 70

Leading-edge flap:
    Area (per side), m² (ft²) 0.048 (0.52)
    Hinge-line location, percent chord 20
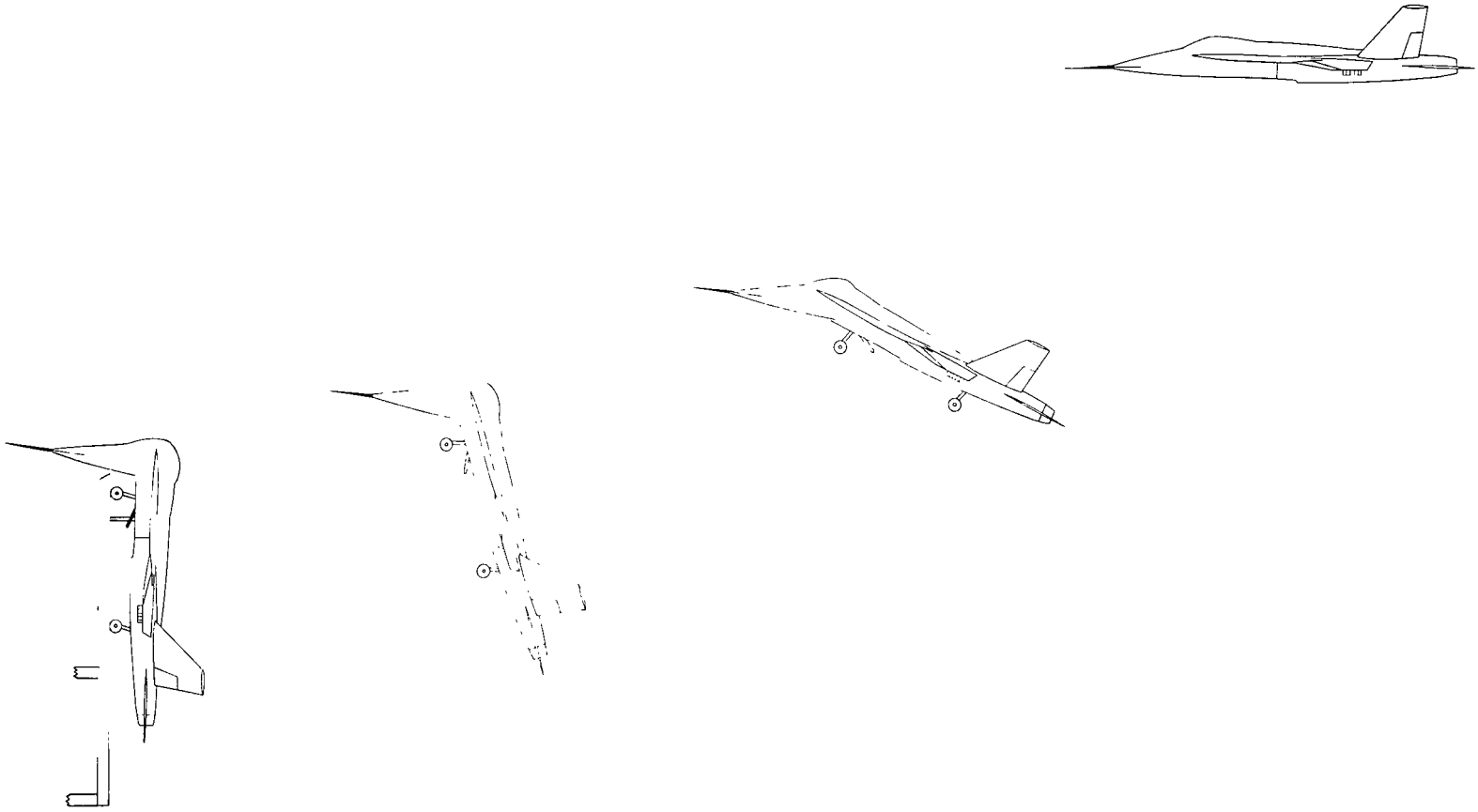
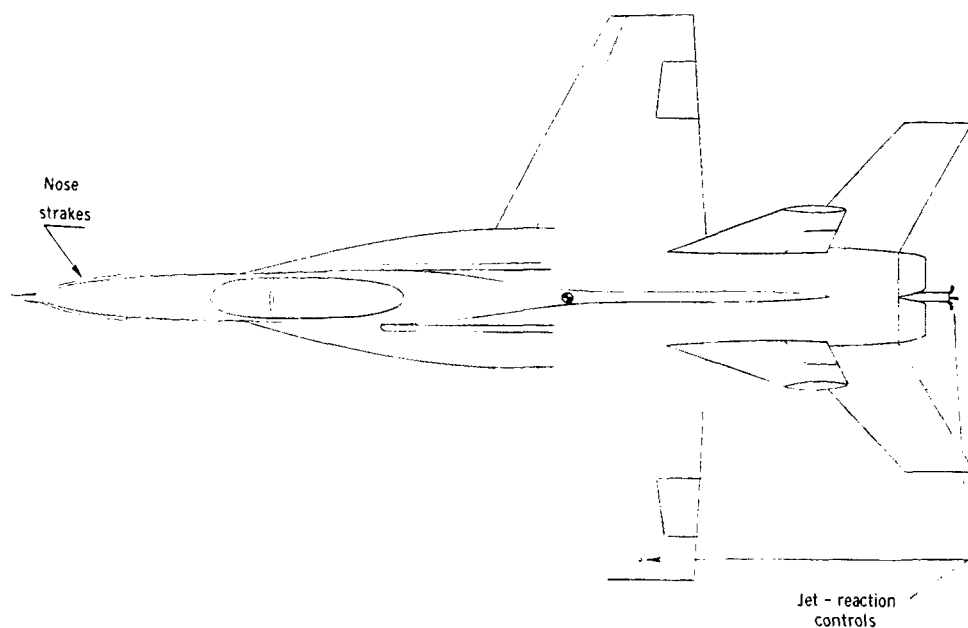Figure 1.- Vertical-attitude VTOL fighter concept.
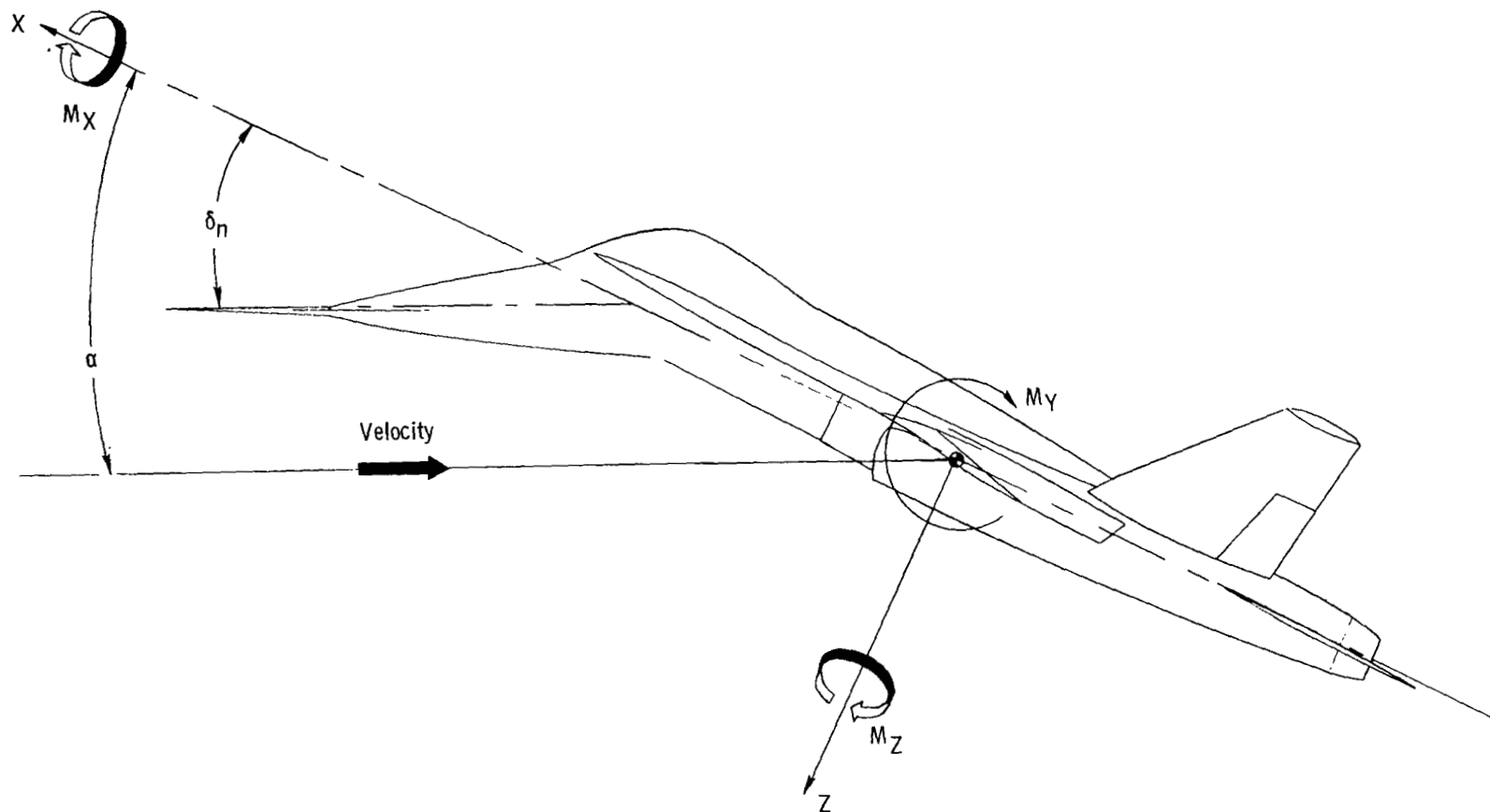
Figure 2.- Body-axis system.

Nose
strakes

Jet – reaction
controls

Nose
pivot

2. 4
(7. 875)

Landing hook

Auxiliary
air intakes

1. 60
(5. 250)
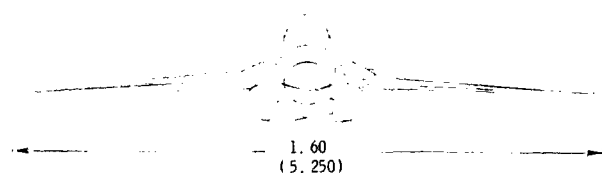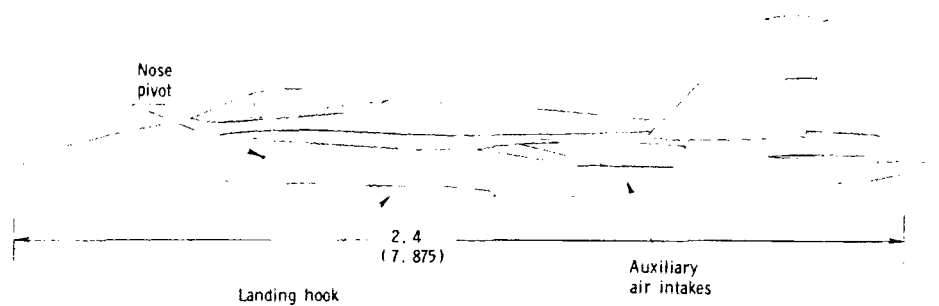
Figure 3.- Three-view sketch of the model.   Dimensions are in meters   (feet).

Pitch and yaw
jet reaction controls
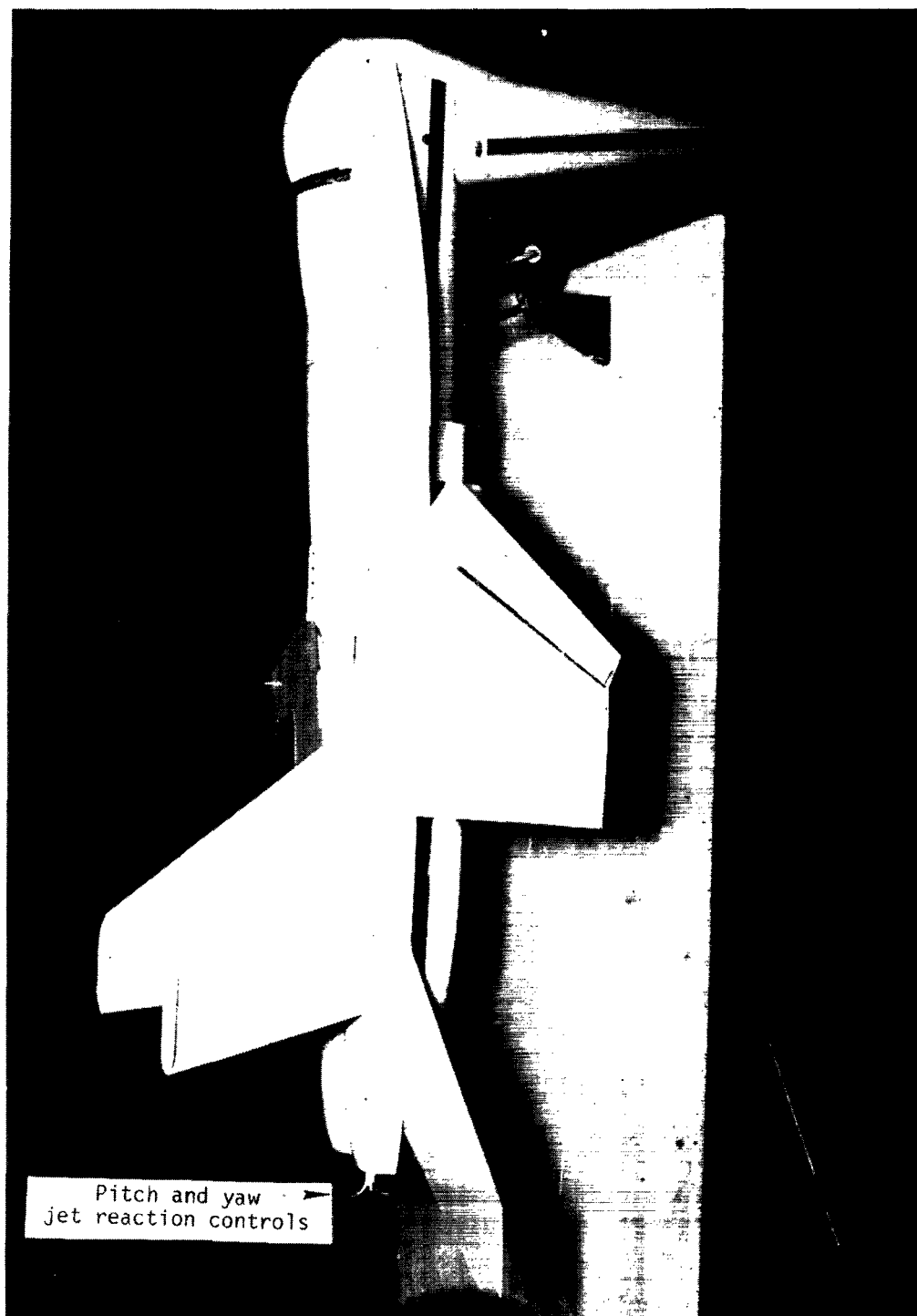
L-75-1259

(a) Hanging on take-off and landing rig.

Figure 4.- Photographs of model used in tests.
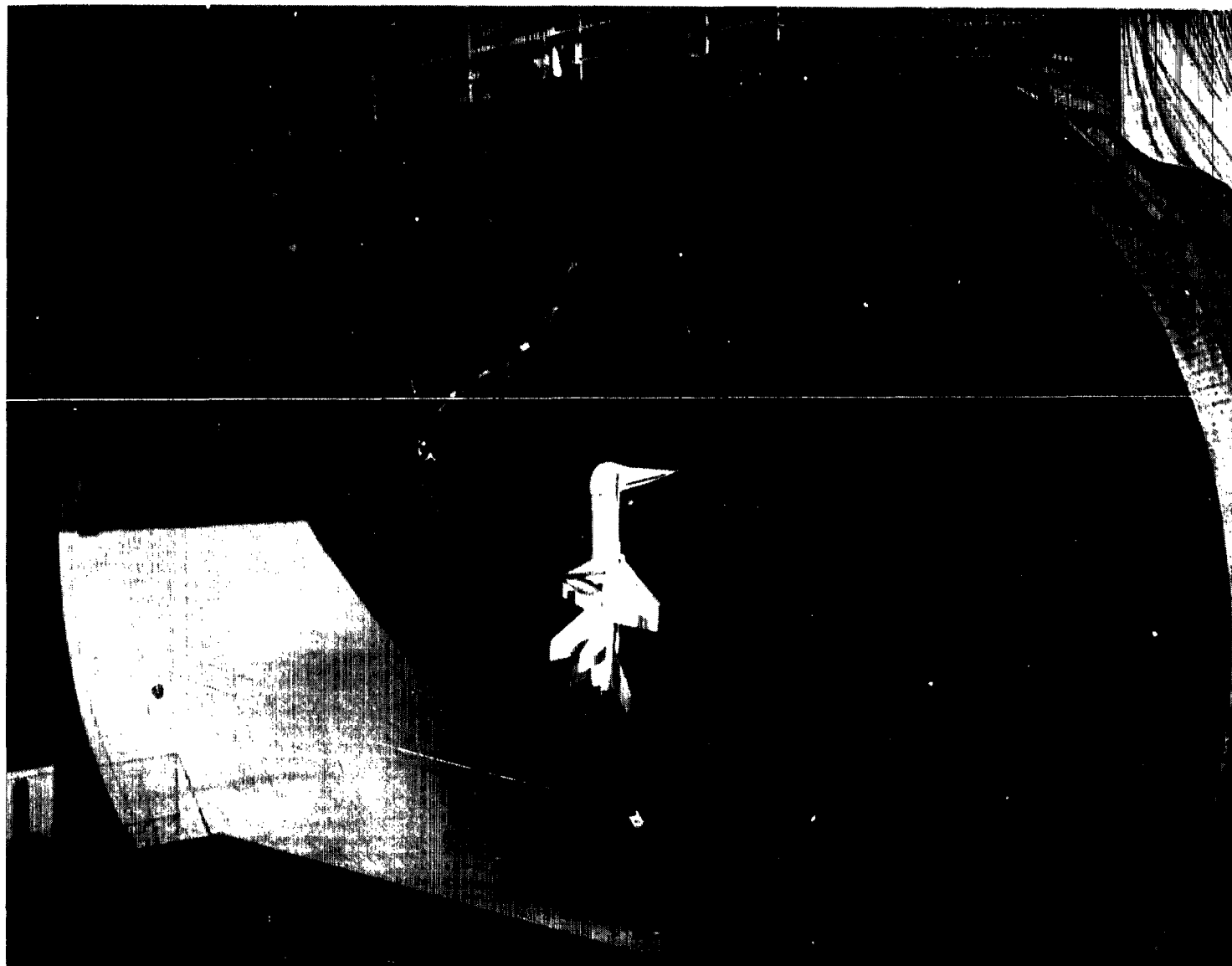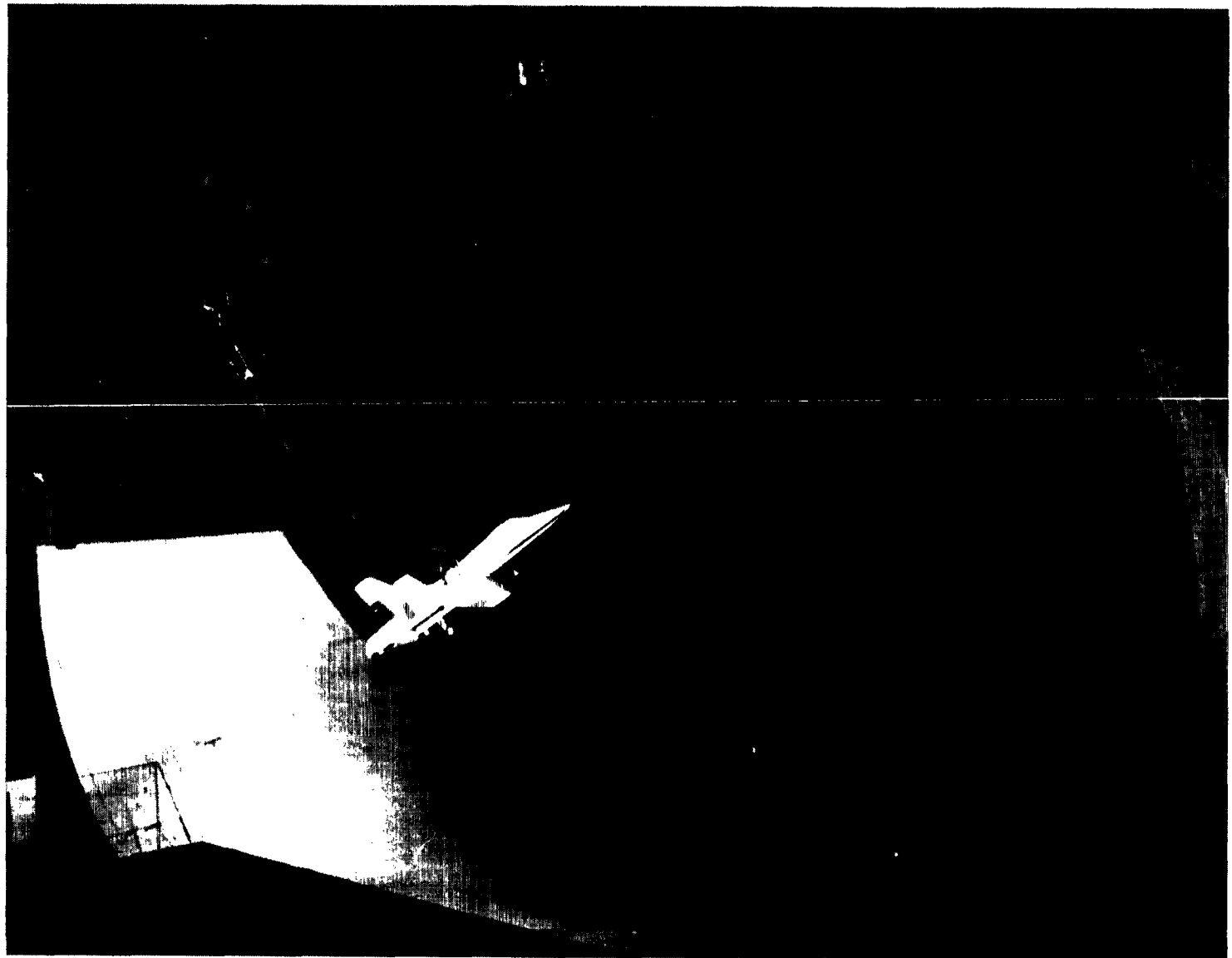
(b) Hovering in Langley full-scale tunnel.

Figure 4.- Continued.
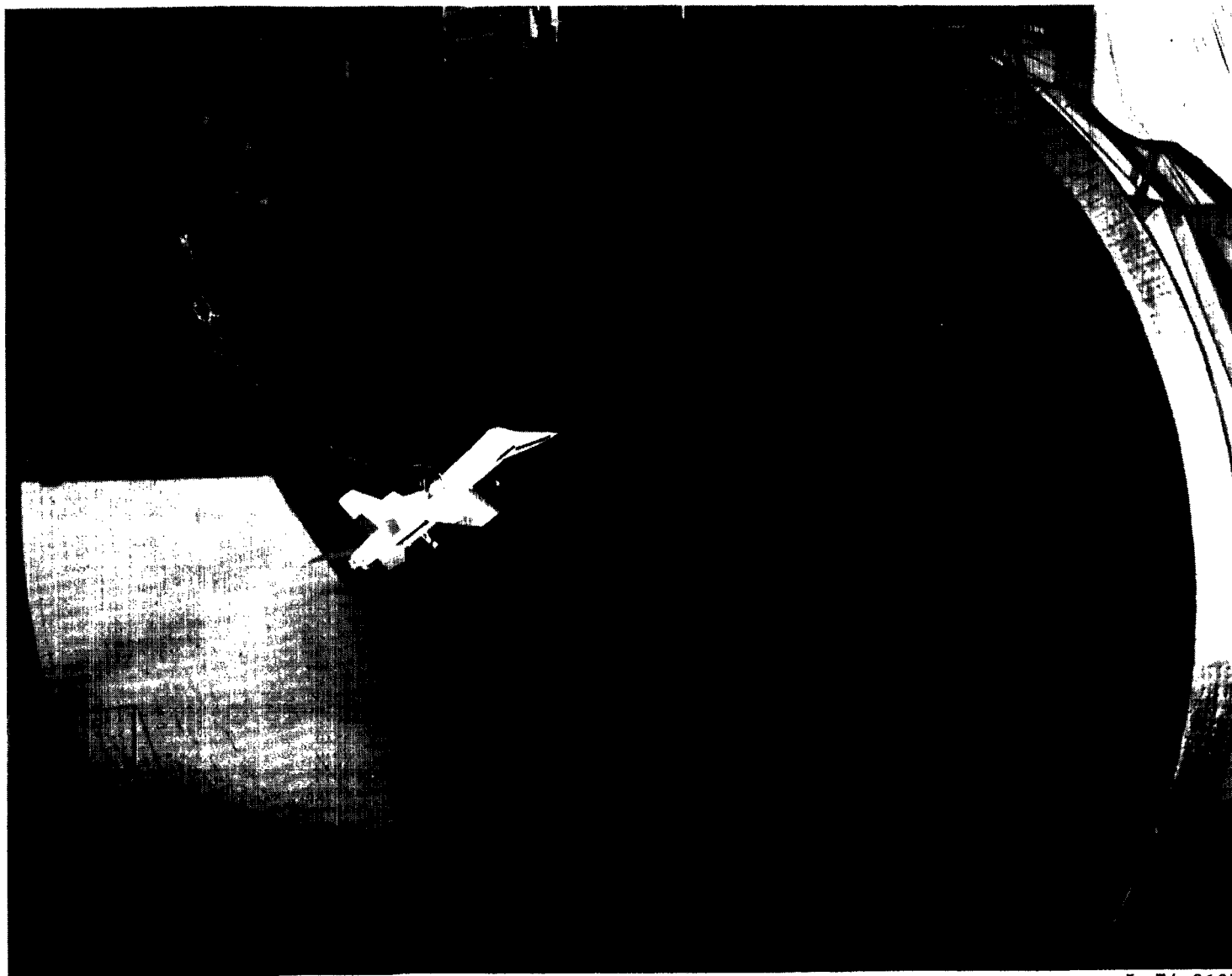
L-74-8197

(c) Midway through transition.

Figure 4.- Continued.

(d) Conventional forward flight.

Figure 4.- Concluded.

POWER AND CONTROL CABLE

SAFETY CABLE

TUNNEL GROUND BOARD

ROLL AND YAW PILOTS

SAFETY-CABLE OPERATOR

POWER OPERATOR

PITCH PILOT
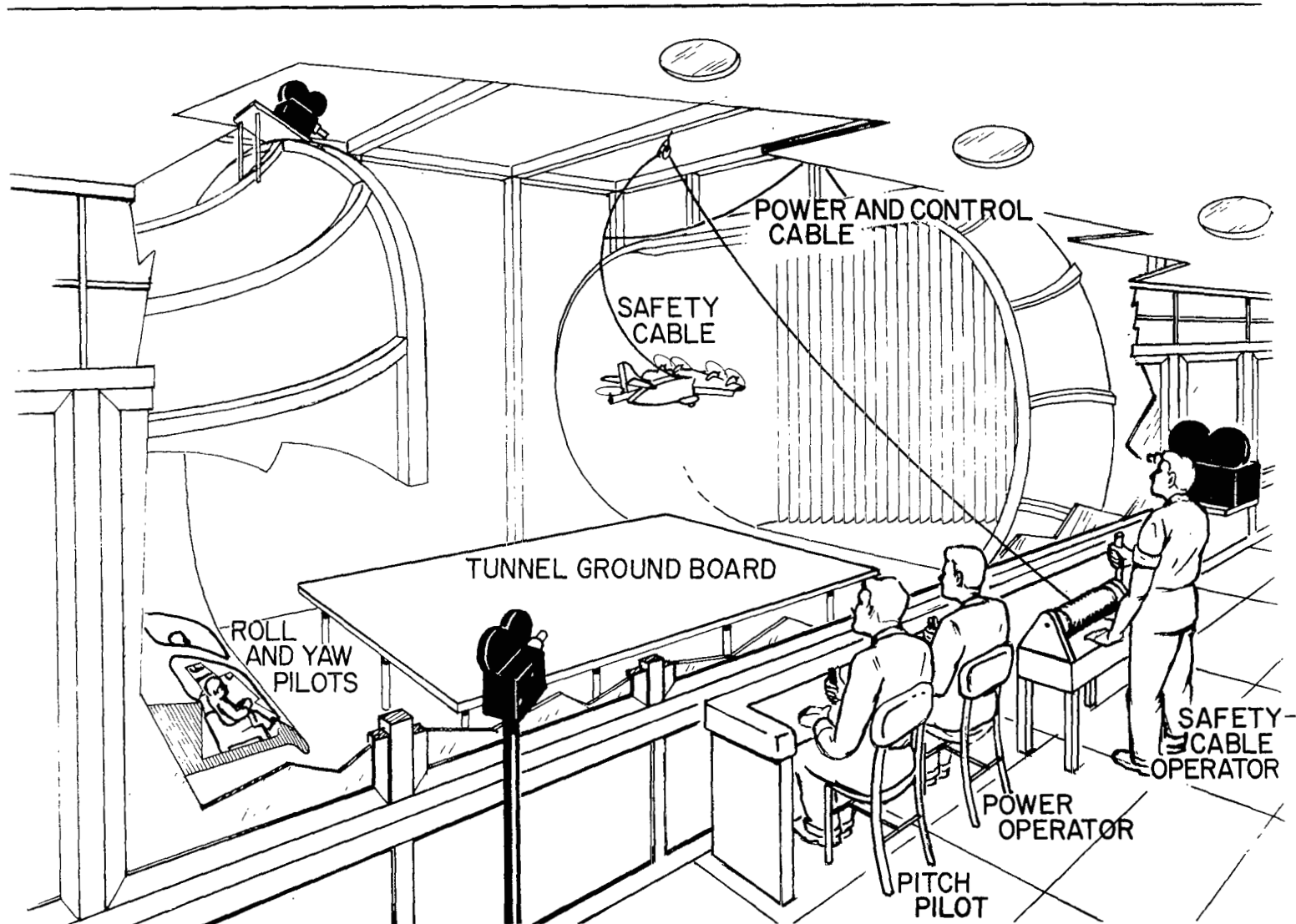
Figure 5.- Test setup for free-flight tests.
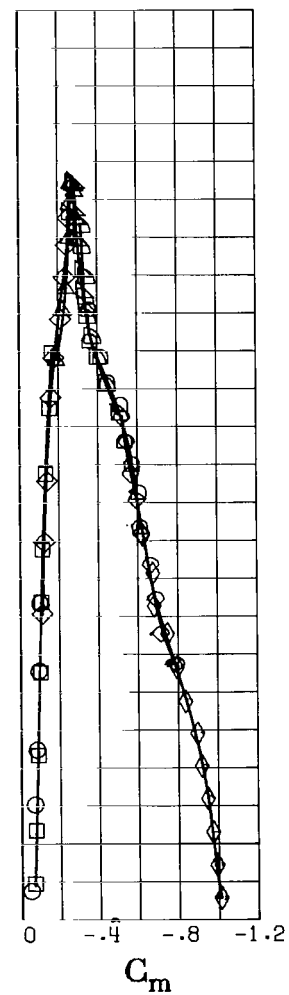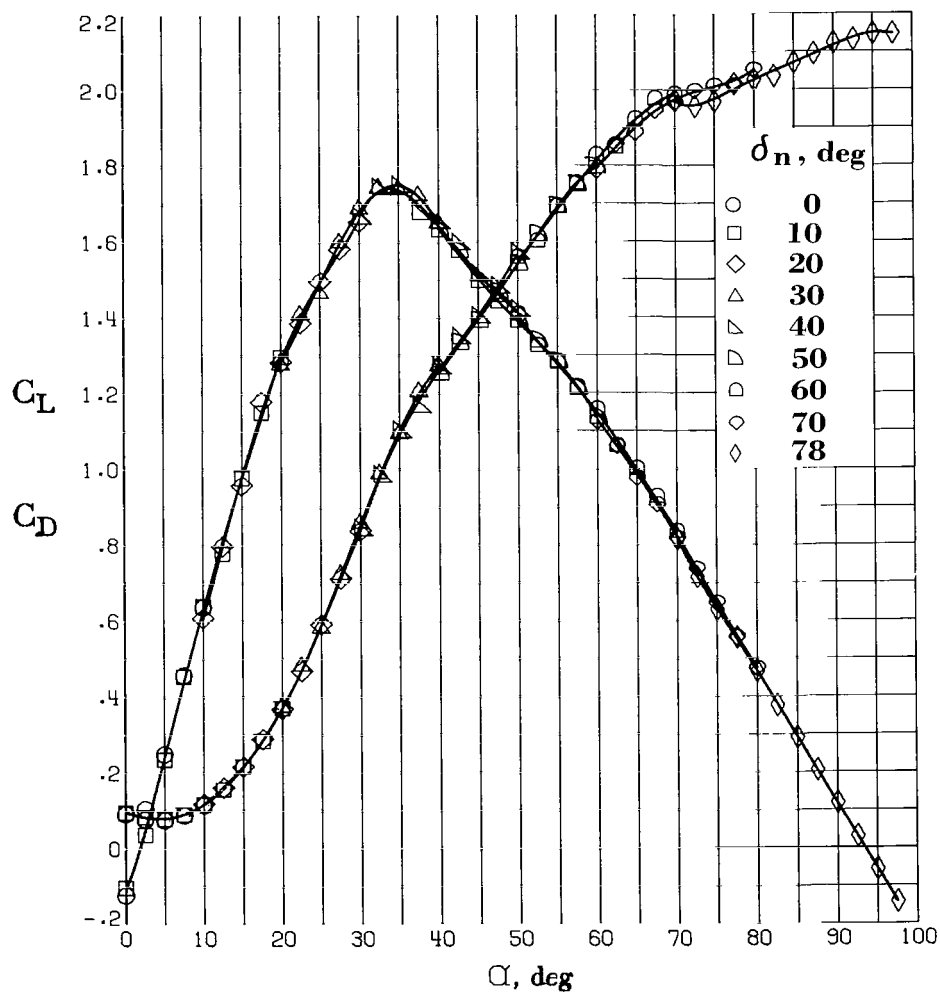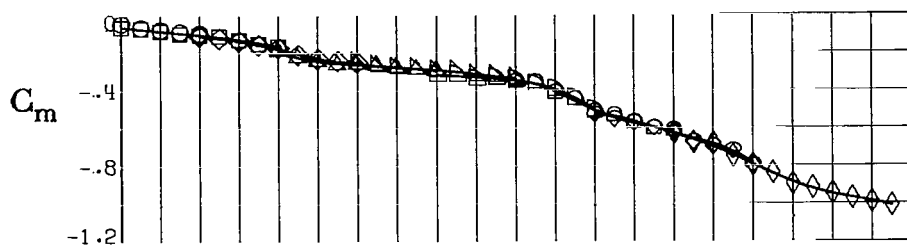
Figure 6.- Effect of fuselage forebody-deflection angle on static longitudinal characteristics of model.
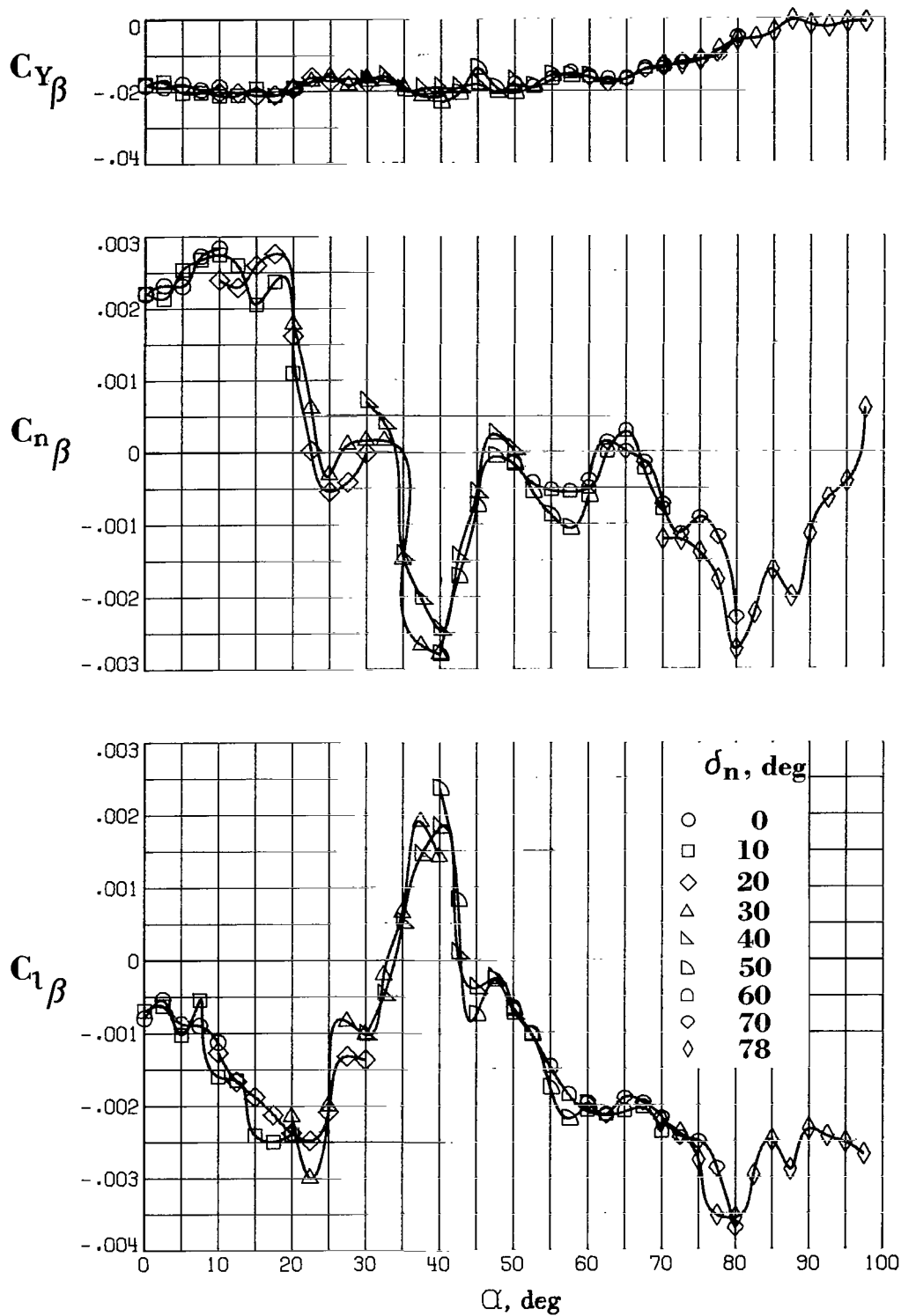
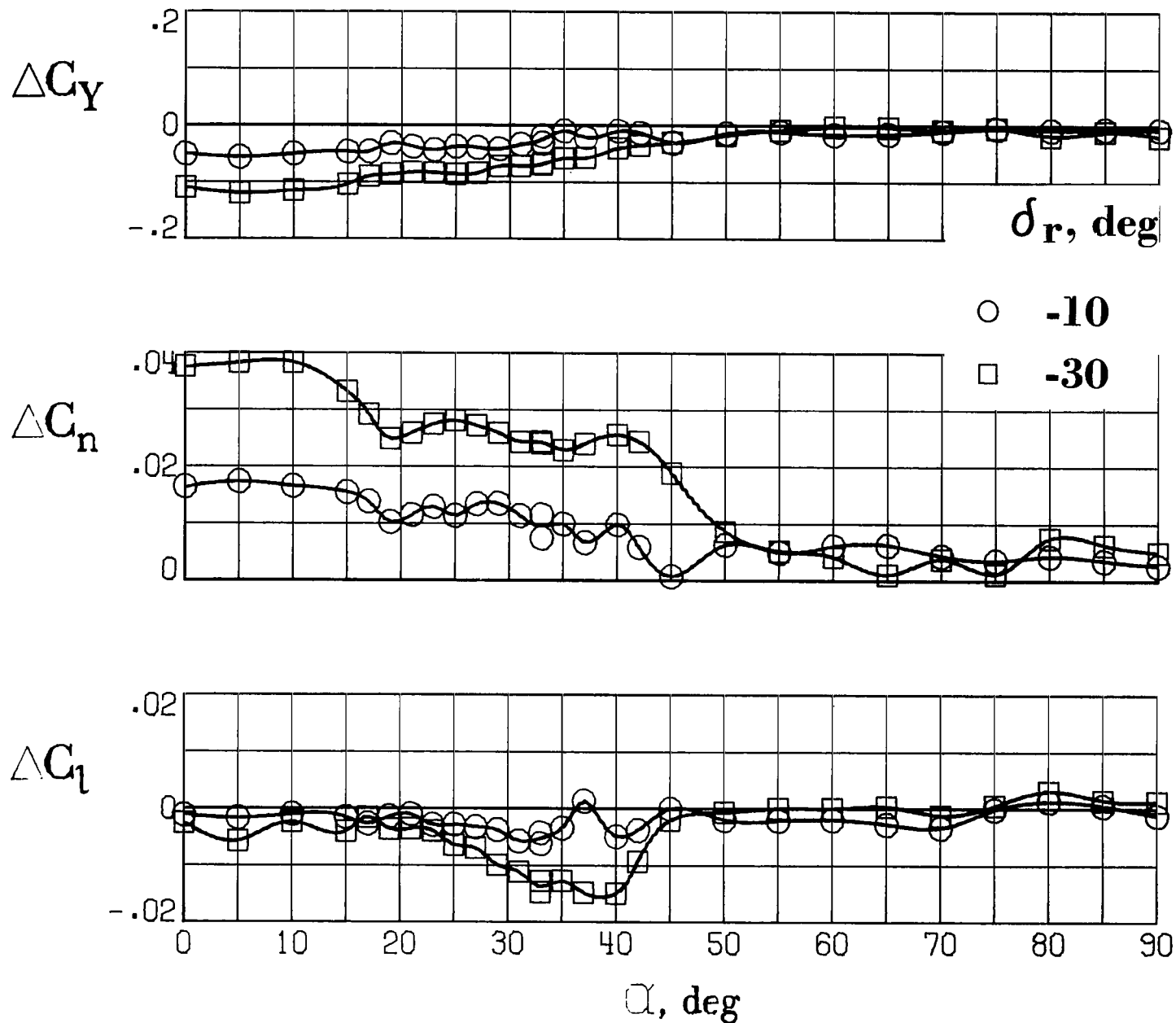Figure 7.- Effect of fuselage forebody-deflection angle on static lateral-directional stability of model.
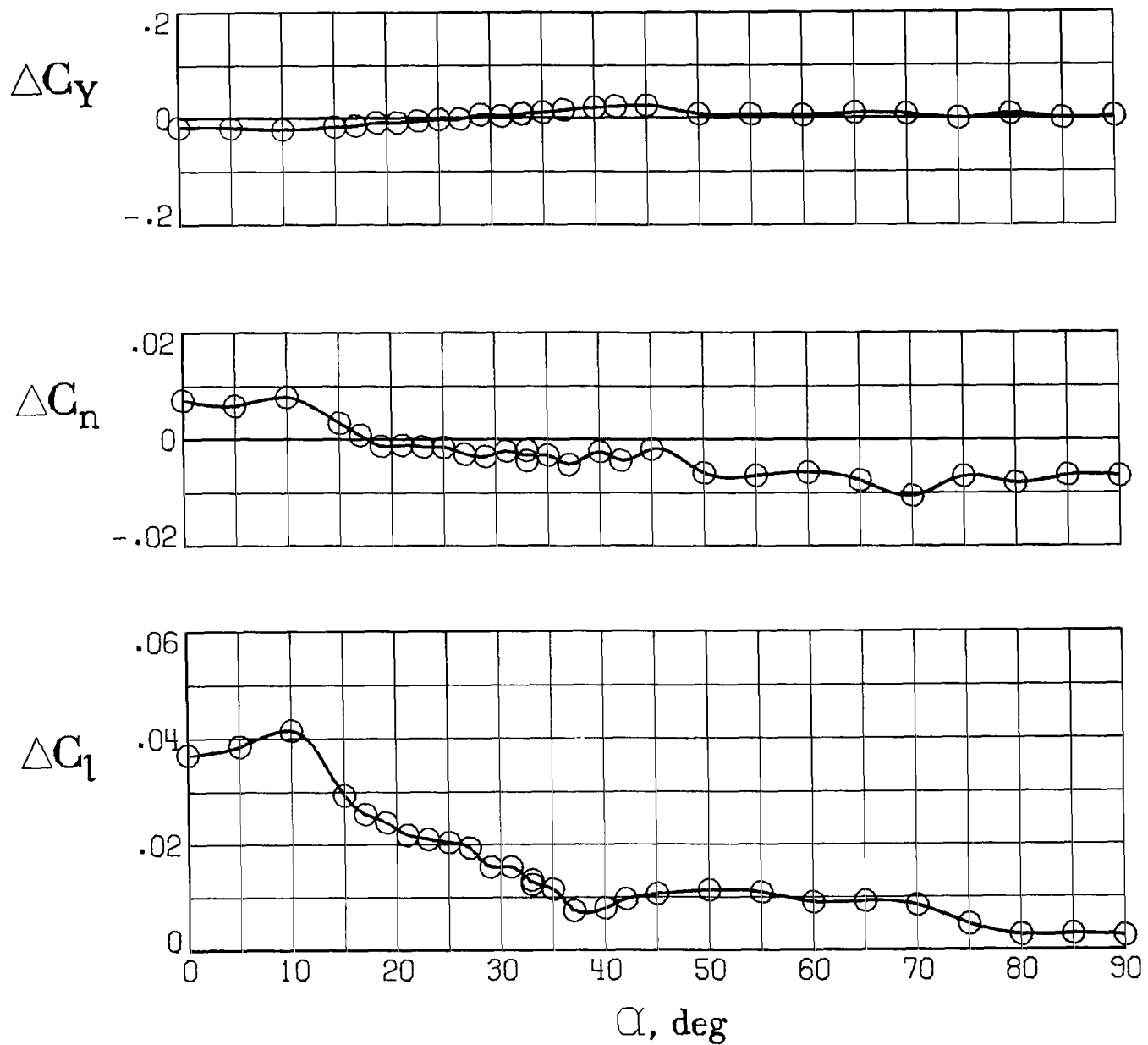
Figure 8.- Effect of rudder deflection. $\delta_n = 0^o$.

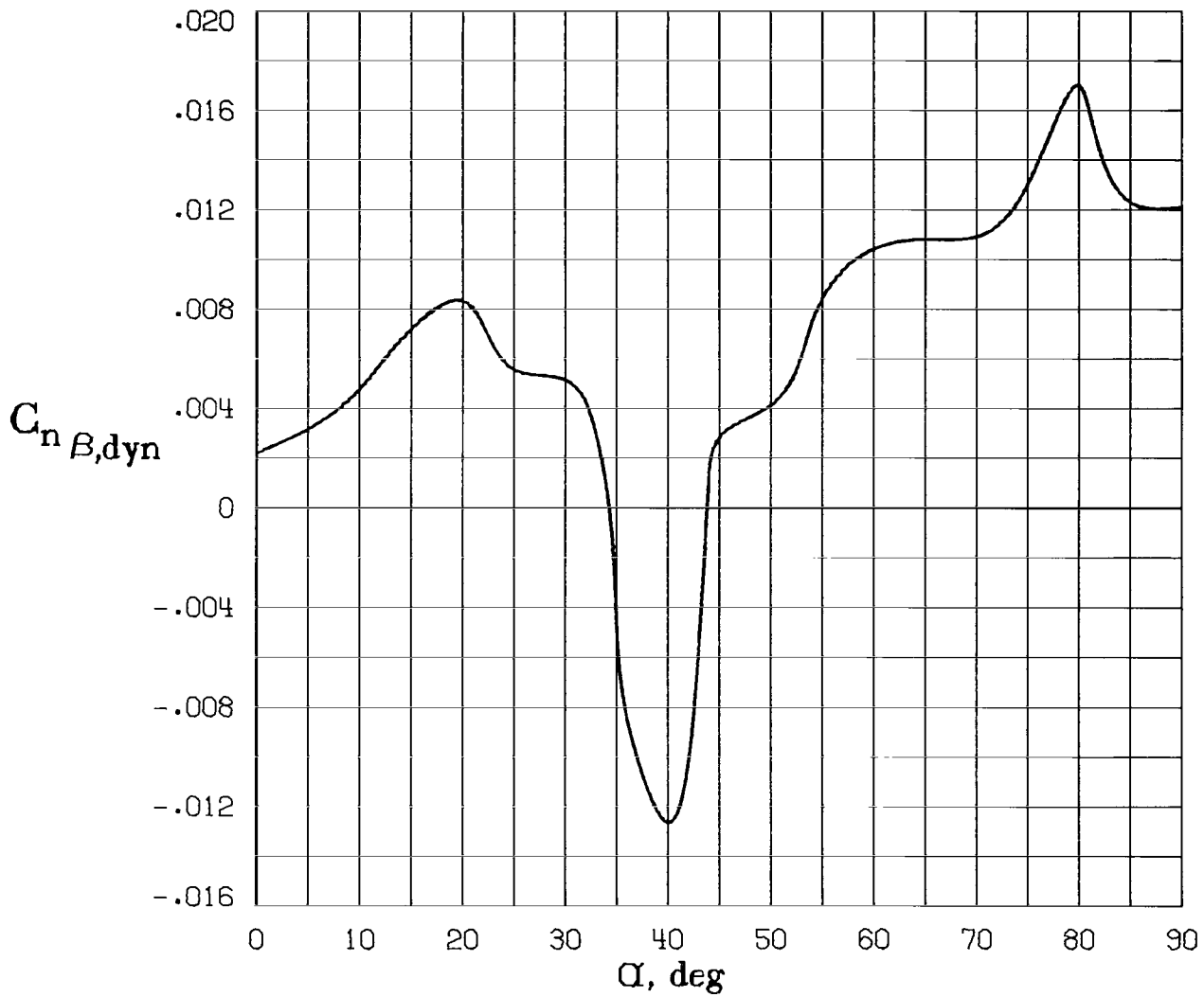Figure 9.- Aileron control effectiveness. $\delta_n = 0^o$; $\delta_a = -30^o$.

Figure 10.- Variation of $C_{n_{\beta},dyn}$ with angle of attack.

A motion-picture film supplement L-1167 is available on loan. Requests will be filled in the order received. You will be notified of the approximate date scheduled.

The film $\left(16 \text{ mm}, 3\frac{3}{4} \text{ min, color, silent}\right)$ shows vertical take-offs, short hovering flights, and transition from hovering to normal forward flight.

Requests for the film should be addressed to:

NASA Langley Research Center
Att: Photographic Branch, Mail Stop 171
Hampton, VA   23665

- - - - - - - - - - - - - - - - - - - CUT - - - - - - - - - - - - - - - -

Date_____

Please send, on loan, copy of film supplement L-1167 to
TN D-8089

Name of organization _____

Street number _____

City and State _____   Zip code

Attention: Mr. ___

Title

CUT

Place
Stamp
Here

NASA Langley Research Center
Att: Photographic Branch, Mail Stop 171
Hampton, VA   23665

003 001 C1 U   A 751017 S00903DS
DEPT OF THE AIR FORCE
AF WEAPONS LABORATORY
ATTN: TECHNICAL LIBRARY (SUL)
KIRTLAND AFB NM 87117

"The aeronautical and space activities of the United States shall be conducted so as to contribute . . . to the expansion of human knowledge of phenomena in the atmosphere and space. The Administration shall provide for the widest practicable and appropriate dissemination of information concerning its activities and the results thereof."
—NATIONAL AERONAUTICS AND SPACE ACT OF 1958

NASA SCIENTIFIC AND TECHNICAL PUBLICATIONS

TECHNICAL REPORTS: Scientific and technical information considered important, complete, and a lasting contribution to existing knowledge.

TECHNICAL NOTES: Information less broad in scope but nevertheless of importance as a contribution to existing knowledge.

TECHNICAL MEMORANDUMS: Information receiving limited distribution because of preliminary data, security classification, or other reasons. Also includes conference proceedings with either limited or unlimited distribution.

CONTRACTOR REPORTS: Scientific and technical information generated under a NASA contract or grant and considered an important contribution to existing knowledge.

TECHNICAL TRANSLATIONS: Information published in a foreign language considered to merit NASA distribution in English.

SPECIAL PUBLICATIONS: Information derived from or of value to NASA activities. Publications include final reports of major projects, monographs, data compilations, handbooks, sourcebooks, and special bibliographies.

TECHNOLOGY UTILIZATION PUBLICATIONS: Information on technology used by NASA that may be of particular interest in commercial and other non-aerospace applications. Publications include Tech Briefs, Technology Utilization Reports and Technology Surveys.

Details on the availability of these publications may be obtained from:

SCIENTIFIC AND TECHNICAL INFORMATION OFFICE

NATIONAL AERONAUTICS AND SPACE ADMINISTRATION
Washington, D.C. 20546